Convergence of shock waves between conical and parabolic boundaries

D. Yanuka, H. E. Zinowits, O. Antonov, S. Efimov, A. Virozub, and Ya. E. Krasik
Physics Department, Technion, Haifa 32000, Israel

(Received 3 May 2016; accepted 7 July 2016; published online 19 July 2016)

Convergence of shock waves, generated by underwater electrical explosions of cylindrical wire arrays, between either parabolic or conical bounding walls is investigated. A high-current pulse with a peak of ~550 kA and rise time of ~300 ns was applied for the wire array explosion. Strong self-emission from an optical fiber placed at the origin of the implosion was used for estimating the time of flight of the shock wave. 2D hydrodynamic simulations coupled with the equations of state of water and copper showed that the pressure obtained in the vicinity of the implosion is ~7 times higher in the case of parabolic walls. However, comparison with a spherical wire array explosion showed that the pressure in the implosion vicinity in that case is higher than the pressure in the current experiment with parabolic bounding walls because of strong shock wave reflections from the walls. It is shown that this drawback of the bounding walls can be significantly minimized by optimization of the wire array geometry. *Published by AIP Publishing.*
[http://dx.doi.org/10.1063/1.4959115]

I. INTRODUCTION

Research of extreme states of matter is important both to basic research and for different applications.[1–4] These extreme states of matter can be obtained using z-pinch, high power lasers, heavy ion beams, and chemical explosives.[5–8] However, these methods require high amounts of stored energy ($\geq 10^5$ J), expensive systems, and large facilities. Recent experimental and numerical research[9] showed that the convergence of a cylindrical shock wave (SW) propagating in water between rigid walls results in pressures of up to 8 GPa at a distance of ~400 μm from the convergence axis when a pulse current using a generator with stored energy of only ~3.6 kJ is applied. In this study, the SWs were generated by underwater electrical explosions of cylindrical wire arrays and propagated between either parabolic or conical shaped walls (see Fig. 1). Application of parabolic shaped boundary walls can lead to a faster decrease in the area of the imploding SW front as compared with a spherical SW implosion resulting in higher pressure behind the SW's front. This approach, i.e., super-spherical implosion, was suggested and studied both analytically and experimentally in earlier research by Chester[10] and Mdivnishvili *et al.*[11] in order to show that the SW implosion in a super-spherical geometry results in higher thermodynamic parameters of the material in the vicinity of implosion. In Ref. 11, the SW was generated in air by a 20 μs duration electrical discharge having toroidal form with a main radius of 50 mm and faster implosion of the SW was obtained in the super-spherical geometry than in the case of the cylindrical one.

Our study's main purpose was to verify that a higher pressure can be obtained in the implosion vicinity with the same amount of stored energy only by changing the shape of the bounding walls. Another purpose was to obtain higher pressure values in the implosion vicinity as compared with that obtained with spherical wire array explosions,[12] which have also attracted great interest in the research of SW.[13] Indeed, it was shown that the pressure in the implosion vicinity is more than 2-fold higher with parabolic walls than with conical walls, because of the faster decrease in the surface area of the SW ($S \propto R_{SW}^3$ for parabolic walls and $S \propto R_{SW}^2$ for conical walls) as it propagates, resulting in a faster increase in its energy density. It was also found that the pressure behind the SW front is higher than in the case of the SW generated by a spherical array explosion, but only for distances >400 μm with respect to the origin. However, at closer distances, the convergence of the SW generated by spherical array results in higher pressure because the SWs are strongly reflected from the parabolic walls.

In this paper, we present the results of similar experiments performed with a generator having a higher stored energy, shorter rise time of the current pulse, and higher peak current. Using a 2D hydrodynamic simulation,[14] the pressure was calculated at a closer distance to the origin, ~50 μm, and further analysis of the SW reflections from the walls was conducted; different wire array geometries were also simulated in order to reduce these SW reflections.

II. EXPERIMENTAL SETUP

The underwater electrical explosions were performed using a high-current generator (stored energy of ~5.4 kJ, rise time of ~300 ns, and peak current of ~550 kA). The current pulse was applied to a 30 mm diameter cylindrical Cu wire array consisting of 60 wires 40 mm in length and 90 μm in diameter. The radius of the wires was chosen to obtain an aperiodic discharge such that most of the stored energy is delivered to them during the explosion. Bounding stainless steel walls (with either conical or parabolic form) were placed in Delrin holders inside the array (see Fig. 1) with a minimal radial distance of 4 mm between the wires and walls. The Delrin holders were used to avoid electrical breakdowns between the high voltage and ground electrodes and the bounding walls. An optical fiber was inserted along the axis through the center of the walls (Fig. 1(a)). When the SW arrived at the fiber, strong self-emission of the fiber was

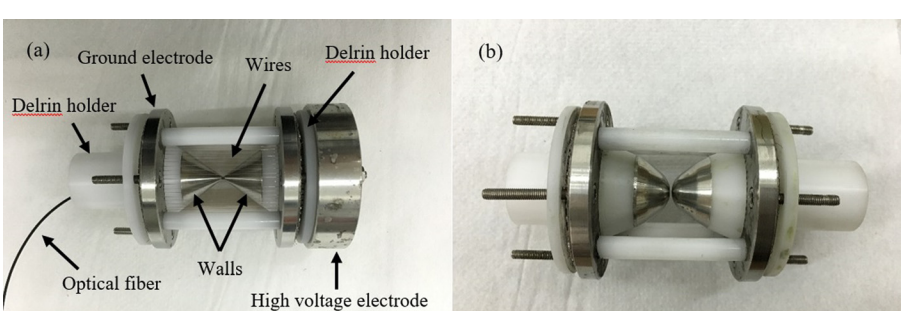

FIG. 1. (a) Cylindrical wire array with conical walls and fiber placed at the axis of the system, before the explosion. (b) Parabolic walls setup after the explosion of wire array.

generated and recorded by a Hamamatsu photomultiplier tube (PMT). The discharge current and voltage were measured by two B-dot and D-dot probes, respectively.

III. EXPERIMENTAL RESULTS

The recorded signals from the B-dot and D-dot probes were integrated and the inductive voltage was subtracted from the total voltage measurement to obtain the resistive voltage $V_R = V_T - V_{ind}$, with a load inductance of ~10 nH. Typical waveforms of the current and resistive voltage and the calculated power and energy are presented in Fig. 2.

The self-emission from the optical fiber for both bounding wall geometries is presented in Fig. 3. The time-of-flight (TOF) of the SW was taken as the time delay between the beginning of the decrease in the discharge current ($t \approx 300$ ns) and the appearance of the strong self-emission of the optical fiber. For each bounding wall geometry, four shots were executed. The TOF of the SW for the conical and parabolic cases are $6.85 \pm 0.003\ \mu$s and $6.46 \pm 0.045\ \mu$s, respectively. This gives a time difference of ~400 ns, which is substantial taking into account that the same amount of energy was initially stored in the pulse generator in these experiments. These TOF data were compared with the results of 2D hydrodynamic simulations.

IV. HYDRODYNAMIC SIMULATION

The pressure in the vicinity of the SW implosion was calculated using 2D hydrodynamic simulations (for detailed description see Ref. 14) based on mass, energy, and momentum conservation laws coupled with the equations of state (EOS) of water and copper.[15] The only input in these simulations is the energy deposition calculated using the recorded discharge current and resistive voltage waveforms. This energy was multiplied by a fitting parameter (<1) to obtain an energy delivery to the converging water flow of ~10% of the total energy initially stored in the pulse generator.[16] There are two main differences between the algorithm described in Ref. 14 and that used in this study: in the present modeling, the symmetry is around the X-axis instead of along the Z-axis (see Fig. 4), as considered in Ref. 14. In addition, instead of the wire explosion modelled in Ref. 14, an electrical explosion of a cylindrical shell having mass equal to the total mass of individual wires was considered. Because of the absence of EOS data for the Delrin material used to hold the bounding walls, it was replaced in the simulation by water because of their similar density ($\rho_w = 1$ g/cm^3 and $\rho_{Delrin} = 1.4$ g/cm^3). In fact, the slightly higher density of Delrin is in some sense compensated by the fact that the stainless steel bounding walls are not completely rigid, as they were considered to be in the simulation.

Typical snapshots of the simulated pressure distribution at $t = 5\ \mu$s (here $t = 0$ is the time corresponding the beginning of the discharge current) are shown in Fig. 4 for both geometries of the bounding walls. Different colors represent different pressure values in the range of *blue* $= 10^5$ Pa and *red* $= 10^9$ Pa. One can see that at this time of implosion the SW converging between parabolic walls already propagates a larger radial distance than that between conical walls. This means also a larger pressure behind the front SW for the case of the parabolic walls. One can also see strong reflections of the SW from the walls; this issue will be addressed in Sec. V.

The temporal evolution of the pressure for both cases of the SW implosion at a radial distance of ~25 μm from the origin is shown in Fig. 5. One can see that the maximal values of pressure of ~11 GPa and ~80 GPa are obtained at $t_{conical} = 7.17\ \mu$s and $t_{parabolic} = 6.76\ \mu$s, respectively, which is in excellent agreement with the experimental results, i.e., $t_{conical} = 7.15\ \mu$s and $t_{parabolic} = 6.76\ \mu$s. Here, $t = 0$ is the beginning of the discharge current. The maximal pressure for the parabolic case is 7.2 times higher than for the conical

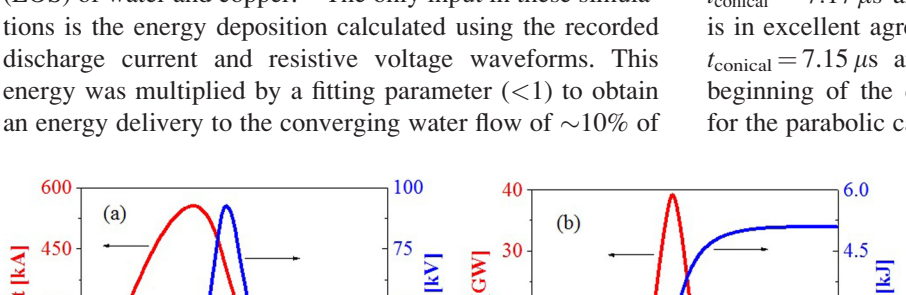

FIG. 2. (a) Current and resistive voltage waveforms. (b) Calculated power and energy.

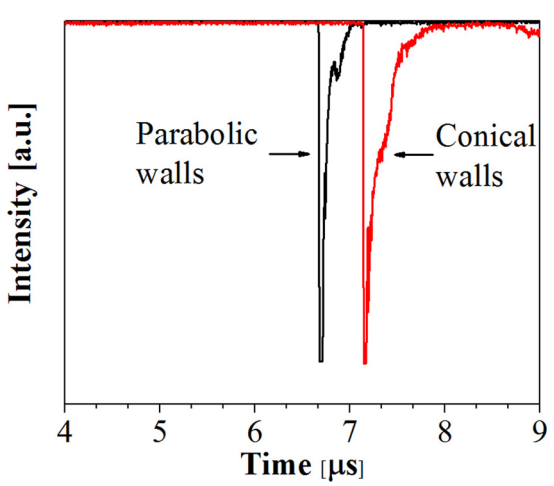

FIG. 3. Self-emission of the optical fiber recorded by the PMT.

case. This result agrees with those described in Ref. 9 and shows clearly that using the same amount of stored energy, one can achieve significantly higher pressure, temperature, and density of water in the vicinity of implosion of the SW converging between parabolic bounding walls. The latter is explained by the faster decrease in the SW's front surface area between parabolic walls, which in turn leads to a faster increase in the SW's energy density, and therefore also to an increase in the water parameters behind the SW front in the vicinity of implosion.

V. DISCUSSION

The results of recent experiments of the underwater electrical explosion of spherical wire arrays and numerical simulations considering SW uniform implosion[12] showed that pressure values up to 10^{12} Pa can be achieved in the vicinity ($r < 5\,\mu$m) of the implosion origin. To draw a comparison with the results of the present research, a 1D numerical simulation for a spherical implosion was performed with the energy density deposition corresponding to the current experiment. In this simulation, the same total mass of the wires was considered and the radius of the spherical array was taken such that the surface area was the same as in the case of the cylindrical wire array. In addition, the energy input in the 1D simulation was adjusted by a fitting parameter to obtain ~10% energy deposition into the water flow, and the average value of the pressure was calculated in the cell closest to the origin having a typical size of 110 μm. Here, let us note that in the case of the 2D simulation of the converging SW between parabolic walls, the size of the triangular cells was significantly smaller, resulting in ~25 cells within the same volume occupied by the cell of 110 μm used in the 1D simulation of the spherical implosion. The calculated average pressure in the case of the spherical implosion was ~130 GPa, which is ~60% higher than the average pressure obtained in 2D simulations for SW implosion between parabolic walls. This result can be explained by strong SW reflections from the walls (see Fig. 4). Earlier research[14,17] has shown that an SW propagating in water without boundaries can self-align azimuthal non-uniformities of its front. This non-uniformity can be caused, for instance, by a slightly different initial radial positions of the array's wires. The uniformity of the SW, which does not occur in the case of the SW propagating between bounding walls because of reflections, is important[18] for the symmetric compression of water in the vicinity of implosion and, consequently, for the generation of high values of pressure, temperature, and density.

To verify this suggestion, a 2D simulation with the same algorithm was performed for the case of a cylindrical wire

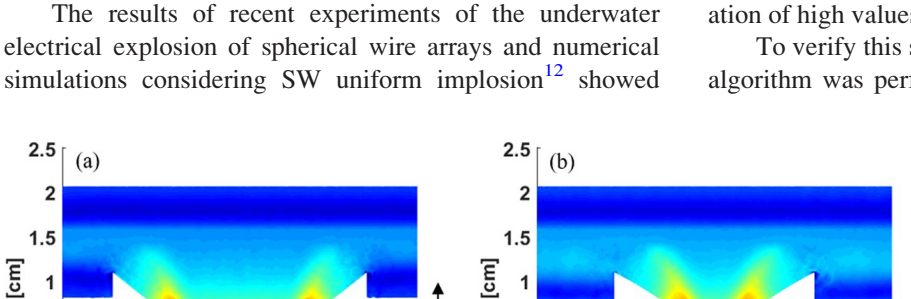

FIG. 4. Snapshots of the pressure distribution in the case of (a) conical walls and (b) parabolic walls at $t = 5\,\mu$s. The colors represent different pressure values, with blue being 10^5 Pa and red 10^9 Pa.

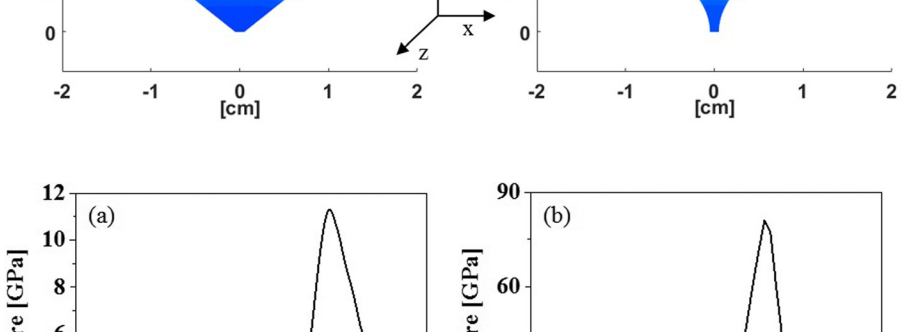

FIG. 5. Temporal evolution of the pressure at a distance of ~25 μm from the origin for (a) conical walls and (b) parabolic walls. Here, $t = 0$ is the time from the beginning of the discharge current.

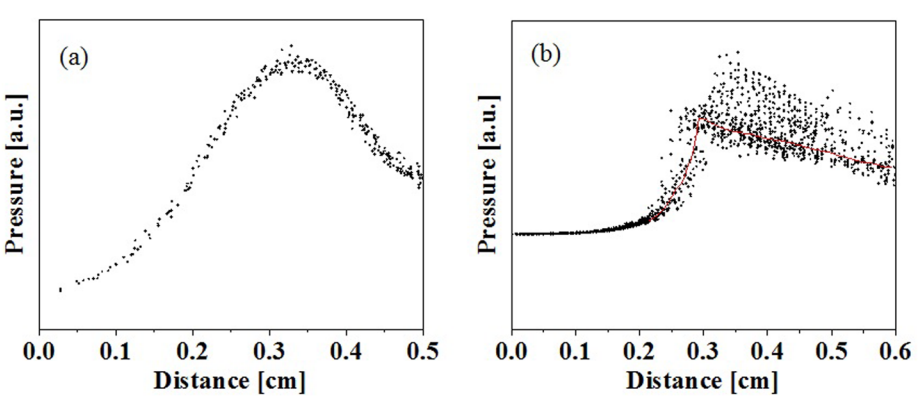

FIG. 6. Scatter plot of the pressure of each triangle in the mesh versus the distance from the origin for (a) no bounding walls and (b) parabolic bounding walls. These plots are obtained at time delays with respect to the beginning of the discharge current $t_{(a)} = 6.8\,\mu$s and $t_{(b)} = 6\,\mu$s.

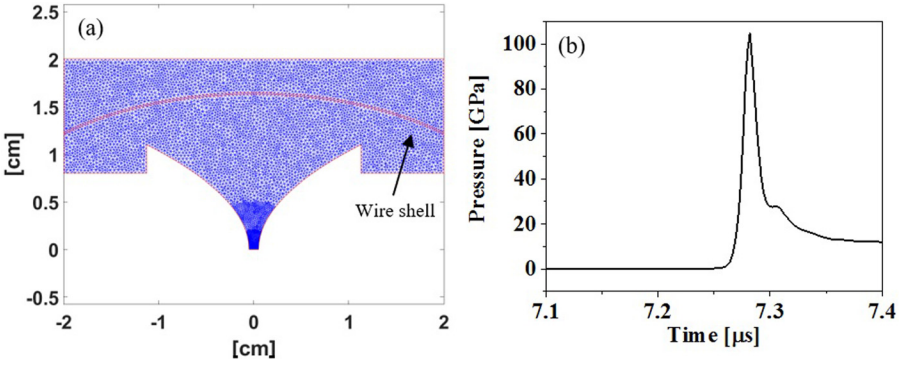

FIG. 7. (a) Triangular mesh of suggested wire array geometry in order to avoid reflections. (b) Temporal evolution of pressure in the implosion vicinity. Here, $t = 0$ is the time from the beginning of the discharge current.

array electrical explosion and generated SW implosion without bounding walls. The area in Fig. 4 is in fact a triangular mesh, with each triangle containing the values of temperature, pressure, and energy density. In the case of the SW propagating without reflections, these values should be approximately the same along the SW front. However, when the SW is reflected from the bounding walls, these values will be not the same along the X-axis for a constant distance from the origin. Scatter plots of the pressure of each triangle in the mesh versus the distance from the origin for the case of cylindrical SW convergence without and with bounding parabolic walls are shown in Fig. 6. Here, each point represents a value of pressure in each triangle at a certain distance from the origin of the SW implosion. One can see that in the cylindrical array case without walls, the values of the pressure at the same distance from the origin are close to each other. However, in the case of the SW convergence between bounding parabolic walls, the pressure values are scattered significantly for the same distance from the origin. This illustrates the non-uniformity of the generated SW front due to the SW reflections from the walls. The red solid line in Fig. 6 represents the approximate profile of the SW without the reflections.

In order to decrease the effect of the SW reflections from the walls one can consider adjusting the wire array geometry in order to generate a converging SW, the front of which is perpendicular in the vicinity of the wall to its surface. 2D simulations were performed for several different wire array geometries and the same total mass of the wires. The results of these simulations showed that indeed adjusting the wire array geometry allows one to increase significantly the pressure in the vicinity of the SW implosion. In Fig. 7(a) one can see the modified geometry of the wire array, which results in an average pressure of $\sim$105 GPa in the volume with a radius of $\sim 50\,\mu$m [see Fig. 7(a)]. This pressure is $\sim$30% larger than that obtained with a cylindrical wire array explosion with parabolic bounding walls, but remains 30% smaller than in the spherical case.

VI. SUMMARY

The results of experiments with sub-microsecond timescale underwater electrical explosions of wire arrays and of numerical simulations showed that, using the same initially stored energy in the pulse generator, one can achieve significantly higher pressure values in the vicinity of the implosion of the SW generated by this explosion and propagating between parabolic bounding walls as opposed to conical walls. However, numerical simulations showed that the values of pressure with parabolic bounding walls, even with modifications of the wire array geometry, are still lower than in the case of a spherical wire array explosion. The reason for the smaller pressure is unavoidable strong SW reflections from the bounding walls. The latter should be considered a serious drawback in the approach where super-spherical SW implosion is applied, and the bounding walls and wire array geometry should be carefully profiled to minimize this effect in order to achieve pressure in the vicinity of the SW convergence comparable with or even larger than that in the spherical geometry.

ACKNOWLEDGMENTS

The authors are grateful to S. Gleizer for technical support and M. Nitishinskiy for fruitful discussions. This research was supported by the Israeli Science Foundation Grant No. 99/12.

[1]T. Ma, P. K. Patel, N. Izumi, P. T. Springer, M. H. Key, L. J. Atherton, L. R. Benedetti, D. K. Bradley, D. A. Callahan, P. M. Celliers, C. J. Cerjan, D. S. Clark, E. L. Dewald, S. N. Dixit, T. Doppner, D. H. Edgell, R. Epstein, S. Glenn, G. Grim, S. W. Haan, B. A. Hammel, D. Hicks, W. W. Hsing, O. S. Jones, S. F. Khan, J. D. Kilkenny, J. L. Kline, G. A. Kyrala, O. L. Landen, S. Le Pape, B. J. MacGowan, A. J. Mackinnon, A. G. MacPhee, N. B. Meezan, J. D. Moody, A. Pak, T. Parham, H. S. Park, J. E. Ralph, S. P. Regan, B. A. Remington, H. F. Robey, J. S. Ross, B. K. Spears, V. Smalyuk, L. J. Suter, R. Tommasini, R. P. Town, S. V. Weber, J. D. Lindl, M. J. Edwards, S. H. Glenzer, and E. I. Moses, Phys. Rev. Lett. **111**, 085004 (2013).
[2]K. K. Reeves and L. Golub, Astrophys. J. Lett. **727**, L52 (2011).
[3]J. J. Rocca, V. Shlyaptsev, F. G. Tomasel, O. D. Cortazar, D. Hartshorn, and J. L. A. Chilla, Phys. Rev. Lett. **73**, 2192 (1994).
[4]R. P. Drake, Phys. Plasmas **16**, 055501 (2009).
[5]I. M. Hall, T. Durmaz, R. C. Mancini, J. E. Bailey, G. A. Rochau, I. E. Golovkin, and J. J. MacFarlane, Phys. Plasmas **21**, 031203 (2014).
[6]B. A. Remington, R. P. Drake, and D. D. Ryutov, Rev. Mod. Phys. **78**, 755 (2006).
[7]N. A. Tahir, D. H. H. Hoffmann, A. Kozyreva, A. Shutov, J. A. Maruhn, U. Neuner, A. Tauschwitz, P. Spiller, and R. Bock, Phys. Rev. E **61**, 1975 (2000).
[8]E. N. Avrorin, B. K. Vodolaga, V. A. Simonenko, and V. E. Fortov, Phys.-Usp. **36**, 5 (1993).
[9]D. Yanuka, M. Kozlov, H. E. Zinowits, and Ya. E. Krasik, Phys. Plasmas **22**, 102708 (2015).
[10]W. Chester, Philos. Mag. **45**, 1293 (1954).
[11]M. O. Mdivnishvili, I. V. Sokolov, M. I. Taktakishvili, and P. A. Voinovich, Shock Waves **9**, 149–158 (1999).
[12]O. Antonov, S. Efimov, D. Yanuka, M. Kozlov, V. Tz. Gurovich, and Ya. E. Krasik, Appl. Phys. Lett. **102**, 124104 (2013).
[13]J. Meyer-ter-Vehn and C. Schalk, Z. Naturforsch. **37a**, 955 (1982).
[14]M. Kozlov, V. Tz. Gurovich, and Ya. E. Krasik, Phys. Plasmas **20**, 112701 (2013).
[15]National Technical Information Service Document No. DE85014241 (S. P. Lyon and J. D. Johnson, Sesame: The Los Alamos National Laboratory Equation-of-State Database, LANL Rep. LA UR-92-3407, 1992). Copies may be ordered from the National Technical Information Service, Springfield, VA, 22161.
[16]O. Antonov, L. Gilburd, S. Efimov, G. Bazalitski, V. Tz. Gurovich, and Ya. E. Krasik, Phys. Plasmas **19**, 102702 (2012).
[17]A. Fedotov, A. Grinenko, S. Efimov, and Ya. E. Krasik, Appl. Phys. Lett. **90**, 201502 (2007).
[18]Th. Lower, R. Sigel, K. Eidmann, I. B. Foldes, S. Huller, J. Massen, G. D. Tsakiris, S. Witkowski, W. Preuss, H. Nishimura, H. Shiraga, Y. Kato, S. Nakai, and T. Endo, Phys. Rev. Lett. **72**, 3186 (1994).